Nucleic Acids Research, 1998, Vol. 26, No. 24 **5699–5706**

Crystal structure of an RNA octamer duplex r(CCCIUGGG)$_2$ incorporating tandem I·U wobbles

Baocheng Pan[1,3], Shome Nath Mitra[1,2], Liqiang Sun[1], David Hart[1] and Muttaiya Sundaralingam[1,2,3,*]

[1]Department of Chemistry and [2]Department of Biochemistry and [3]Biophysics Program, The Ohio State University, Biological Macromolecular Structure Center, Columbus, OH 43210, USA

Received July 14, 1998; Revised and Accepted October 29, 1998

ABSTRACT

The crystal structure of the RNA octamer duplex r(CCCIUGGG)$_2$ has been elucidated at 2.5 Å resolution. The crystals belong to the space group $P2_1$ and have unit cell constants *a* = 33.44 Å, *b* = 43.41 Å, *c* = 49.39 Å and β = 104.7° with three independent duplexes (duplexes 1–3) in the asymmetric unit. The structure was solved by the molecular replacement method and refined to an R_{work}/R_{free} of 0.185/0.243 using 3765 reflections between 8.0 and 2.5 Å. This is the first report of an RNA crystal structure incorporating I·U wobbles and three molecules in the asymmetric unit. Duplex 1 displays a kink of 24° between the mismatch sites, while duplexes 2 and 3 have two kinks each of 19° and 27°, and 24° and 29°, respectively, on either side of the tandem mismatches. At the I·U/U·I mismatch steps, duplex 1 has a twist angle of 33.9°, close to the average for all base pair steps, but duplexes 2 and 3 are underwound, with twist angles of 24.4° and 26.5°, respectively. The tandem I·U wobbles show intrastrand purine-pyrimidine stacking but exhibit interstrand purine-purine stacking with the flanking C·G pairs. The three independent duplexes are stacked non-coaxially in a head-to-tail fashion to form infinite pseudo-continuous helical columns which form intercolumn hydrogen bonding interactions through the 2′-hydroxyl groups where the minor grooves come together.

INTRODUCTION

Inosine (I) is an analog of guanosine without the 2-amino group and it is found in the first position of some tRNA anticodons (1,2), double-stranded RNAs (dsRNA) (3,4), mRNAs (5–8) and viral RNAs (9–12). Crick has proposed that tRNA molecules with guanosine/inosine in the anticodon can translate mRNA codons ending in uridine (G·U/I·U wobble), cytidine (G·C/I·C) and adenosine (G·A/I·A) (13). G·U pairs are by far the most stable amongst different mismatches and occur most frequently in biological RNAs. Some of the G·U pairs are invariant in rRNAs while others may be replaced by an A·C wobble, which we now know is A^+·C (14,15), and I·U or Watson–Crick base pairs (16–18). Due to recognition of G·U pairs by proteins, attempts have been made to investigate the contribution of the appended atoms in RNA function (19). Thermodynamic studies have shown that G·U is slightly more stable than I·U at the terminus but much more stable in the interior of a duplex (19). Also, the A·U pair is slightly more stable than a G·U pair and it is significantly more stable than an I·U pair (19,20). To understand the conformational details of the I·U pair in RNA, we have studied the crystal structure of tandem I·U/U·I pairs in the octamer r(CCCIUGGG). The presence of three independent duplexes in the asymmetric unit provides the opportunity to study the I·U/U·I mismatches under different local environments and to observe the conformational flexibility of the RNA duplex. The geometry of the tandem I·U/U·I wobble pairs in motif II using the nomenclature below and their effects on the overall structure of RNA duplexes have been compared with other tandem wobbles; G·U/U·G(21), referred to as motif II, and U·G/G·U(22), referred to as motif I. Tandem C·A^+/A^+·C pairs (15), in motif I using the above nomenclature, have recently been determined in crystal and they have also been compared. All the tandem wobbles were determined as octamers.

MATERIALS AND METHODS

Synthesis of inosine phosphoramidite

The protected inosine phosphoramidite is not available commercially and was synthesized according to pathway 'A' in the method described by Green *et al*. (23). A step gradient of eluting solvents was used in silica gel chromatography instead of a fixed concentration. Progress of the synthesis was monitored by comparing the NMR spectra at different stages. The orange color of the released trityl group indicated efficient coupling for the oligonucleotide synthesis.

Oligonucleotide synthesis and purification

The RNA octamer r(CCCIUGGG) was synthesized by the phosphoramidite method using an in-house Applied Biosystem DNA synthesizer 391. The RNA was cleaved from the solid support using 5 ml ammonium hydroxide (30% NH_3 in water) in 30% ethanol. The 3′-hydroxyl group was deprotected in the same solution at 55°C overnight. The sample was lyophilized by dissolving in 0.8 ml tetrabutylammonium fluoride for 6 h at room temperature to deprotect the 2′-hydroxyl group and then lyophilized

*To whom correspondence should be addressed at: Department of Chemistry, The Ohio State University, 012 Rightmire Hall, Carmack Road, Columbus, OH 43210, USA. Tel: +1 614 292 2925; Fax: +1 614 292 2524; Email: sundaral@chemistry.ohio-state.edu

again in 0.8 ml of 0.1 M triethylamine acetate. The sample was precipitated using 100% ethanol in the presence of 2.5 M ammonium acetate at –25°C for 4 h and then purified by ion-exchange FPLC using LiCl for the eluting gradient. LiCl was used as the eluant because it does not precipitate with ethanol so the sample can be desalted during ethanol precipitation. Ethanol precipitation and lyophilization were carried out until a white fluffy material was obtained. For crystallization a stock solution of 2 mM single-stranded octamer was prepared in distilled water.

Crystallization and data collection

The crystallization was carried out by the hanging drop vapor diffusion method at room temperature. The best crystals were obtained in several days using 1 mM RNA (single-strand concentration) in the presence of 50 mM sodium cacodylate buffer (pH 5.0), 10 mM magnesium chloride, 25 mM spermine tetrachloride and 2.4% 2-methyl-2,4-pentanediol (MPD), equilibrated against a reservoir of 1 ml of 40% MPD. A crystal of dimensions 0.2 × 0.2 × 0.1 mm was mounted in a thin-walled glass capillary with mother liquor at one end and sealed with wax. The intensity data were collected at room temperature using an in-house R-AXIS IIc imaging plate and a 50 kV/100 mA graphite monochromated CuK_α X-ray beam. The crystal-to-detector distance was 10.0 cm and 4156 independent reflections up to 2.5 Å resolution (87.4% completeness) were collected with an R_{merge} of 0.048. Of these, 3912 reflections had $F \geq 2\sigma(F)$ (79.9% complete). There were 61% of the data in the highest resolution bin of 2.6–2.5 Å. The crystals were stable in the X-ray beam during the entire course of data collection. The data were processed using the software v.2.1 from the manufacturer (Molecular Structure Corporation). Crystal data are summarized in Table 1.

Table 1. Crystal data and refinement parameters for $r(CCCIUGGG)_2$

Space group	$P2_1$
a (Å)	33.44
b (Å)	43.41
c (Å)	49.39
β (°)	104.7
Asymmetric unit	3 duplexes
Volume/bp (Å^3)	1400
Resolution range (Å)	8.0–2.50
Number of reflections used [$F \geq 2.0\sigma(F)$]	3765
Final R_{work}/R_{free} (%)	18.5/24.3
Final model	
Nucleic acid atoms	1008
Water molecules	26
Average thermal parameters (Å^2)	
Nucleic acid atoms	30.8
Water molecules	42.6
Parameter file	param_nd.dna
r.m.s. deviation from ideal geometry	
Bond lengths (Å)	0.005
Bond angles (°)	1
Dihedral angles (°)	8
'Improper' angles (°)	1

Structure solution and refinement

The structure of the octamer r(CCCIUGGG) was solved by the molecular replacement method using the program AMoRe (24). The search model used was the octamer r(CCCCGGGG) (25) (NDB accession no. ARH064). Rotation–translation searches were performed with 3765 reflections [$F \geq 2\sigma(F)$] in the resolution range 8.0–2.5 Å. The highest peak had a correlation coefficient of 43.5% and an R-factor of 52.2% for the position of the first duplex. Fixing the duplex in this position, the second duplex was searched and the highest peak gave a correlation coefficient of 58.7% and R-factor of 45.6%. The two helices packed in the unit cell leaving enough space to accommodate another octamer duplex. This prompted a search for the third duplex, which was achieved by fixing the first two duplexes and performing a translation search. The highest set of peaks gave a correlation coefficient of 70.1% and an R-factor of 0.392. The result was supported by the fact that the volume/bp was 1400 Å^3 for three independent duplexes (referred to as duplex 1, duplex 2 and duplex 3) and the packing had no short contacts.

As the ratio of reflections to parameters was low, the refinement was initially started using non-crystallographic symmetry (NCS) restraints as implemented in X-PLOR (26). Duplexes 1 and 2 are related by NCS and both are related to duplex 3 by an ~2-fold symmetry. Rigid body refinement with 3765 reflections [$F \geq 2\sigma(F)$] in the resolution range 8.0–2.5 Å brought the R_{work}/R_{free} to 0.413/0.418. After several cycles of Powell conjugate gradient energy minimization, the R_{work}/R_{free} converged to 0.343/0.376. Refinement was continued by simulated annealing and the R_{work}/R_{free} dropped only to 0.314/0.384. The $2|F_o|–|F_c|$ map showed that many regions of the structure were not clear and, coupled with high values for R_{work}/R_{free} at this stage of refinement, indicated that the three independent duplexes might be conformationally different. Therefore, the NCS restraints were removed and the three duplexes were allowed to refine freely. Positional refinement dropped the R_{work}/R_{free} to 0.265/0.333. In accordance with the omit $|F_o|–|F_c|$ maps, the central 2 bp in the three duplexes were replaced to conform to the correct sequence. Refinement of the corrected model by simulated annealing and application of individual B factors dropped the R_{work}/R_{free} to 0.208/0.260. In all, 26 water molecules were located and further refinement gave a final R_{work}/R_{free} of 0.185/0.243. The final model contains 1008 nucleic acid atoms and 26 water molecules. The crystal data and refinement statistics are summarized in Table 1. The atomic coordinates and the structure factors have been deposited with the Nucleic Acid Database (27) (NDB accession no. AR0004).

RESULTS AND DISCUSSION

The octamer duplex

The three independent duplexes in the asymmetric unit with their numbering scheme are shown in Figure 1. The helical parameters of the duplexes are shown in Table 2. The octamer r(CCCIUGGG) crystallizes in the A-RNA form with a global helical twist of 34.9° and a helical rise of 2.47 Å for duplex 1, 32.3° and 2.58 Å for duplex 2 and 32.7° and 2.72 Å for duplex 3. All the sugar puckers are in the C3′-*endo* conformation except C1 in duplex 2 and C11 in duplex 3, which are in the C2′-*exo* conformation, closely related to C3′-*endo* conformation. The octamers contain three Watson–Crick C·G/G·C base pairs flanking the tandem I·U/U·I wobbles in the middle. The three

independent duplexes are stacked non-coaxially in a pseudo-continuous fashion. A superimposition of the three independent duplexes gives an r.m.s. deviation of 1.24 Å for duplexes 1 and 2, 1.45 Å for duplexes 1 and 3 and 0.55 Å for duplexes 2 and 3. Thus, duplexes 2 and 3 resemble each other more closely and differ from duplex 1. The major conformational differences in duplex 1 are in the phosphates of C3, I4, C11 and I12 with an average r.m.s. deviation of 2.28 Å.

Table 2. Helical parameters of r(CCCIUGGG)

Base pair	Twist (°)	Rise (Å)	Roll (°)	Tilt (°)	Prop (°)	Buckle (°)
Duplex 1						
C1·G16					–3.97	–5.44
	35.97	2.48	–5.18	–0.66		
C2·G15					–3.21	–1.34
	29.76	2.37	1.02	1.70		
C3·G14					–1.75	0.83
	32.48	2.31	–4.67	–0.41		
I4·U13					–5.55	11.75
	31.96	2.84	–3.02	1.44		
U5·I12					–3.39	–0.14
	39.90	2.62	–0.54	–0.08		
G6·C11					–8.14	0.72
	31.54	2.28	–7.93	–0.93		
G7·C10					–9.52	7.06
	35.38	2.41	–7.94	–0.17		
C8·G9					–1.04	–1.27
Average	33.85	2.47	–4.04	0.13	–4.57	1.52
Duplex 2						
C1·G16					–1.21	–1.16
	31.37	2.58	–7.01	–3.66		
C2·G15					–3.98	–3.74
	35.80	2.53	–2.05	0.44		
C3·G14					–1.35	0.55
	33.24	2.71	3.64	4.35		
I4·U13					–5.38	3.61
	24.40	2.35	–4.16	0.32		
U5·I12					–3.96	0.79
	34.34	2.79	–4.54	–5.24		
G6·C11					0.34	2.71
	32.52	2.69	–4.53	0.93		
G7·C10					–3.19	1.89
	34.58	2.41	0.74	–0.39		
C8·G9					–2.73	3.29
Average	32.32	2.58	–2.56	–0.46	–2.68	0.99
Duplex 3						
C1·G16					–1.23	–4.13
	35.57	2.63	1.03	–3.39		
C2·G15					–4.04	–2.61
	35.55	3.02	1.59	0.45		
C3·G14					–1.76	0.41
	24.07	2.51	–4.39	4.76		
I4·U13					–0.64	4.43
	26.49	2.54	0.88	0.82		
U5·I12					–0.23	–3.48
	39.92	2.75	–10.76	–4.33		
G6·C11					–2.09	–0.01
	33.1	3.02	7.04	2.65		
G7·C10					–2.81	–3.03
	35.85	2.61	2.33	2.96		
C8·G9					–7.62	4.15
Average	32.65	2.72	–0.33	0.56	–2.55	–0.53

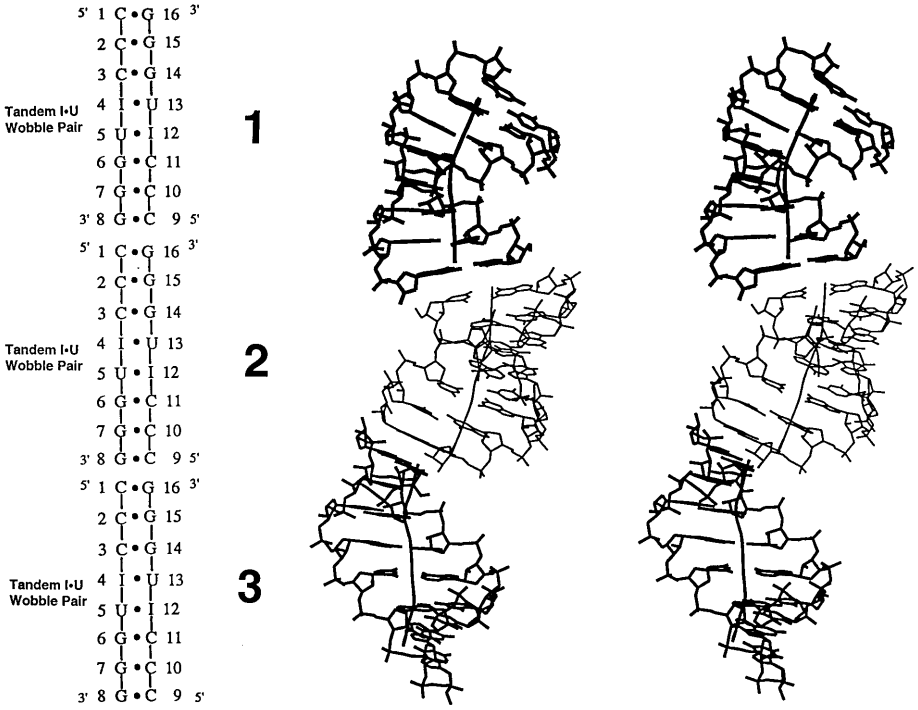

Figure 1. Stereoview of the three duplexes showing the bends in the helices and the numbering scheme.

The helical axes of the three duplexes are bent. The program CURVES (28) was used to calculate the helical axes of the duplexes. For a clear visualization of the bending angles, the three independent duplexes with their curved helical axes are superimposed on fiber A-RNA (Fig. 2). The end-to-end bending angle for duplex 1 is 4.0° while in duplexes 2 and 3 they are 8.8° and 10.3° respectively. This indicates that the end-to-end bending in the molecules is not pronounced but the local kinks (24° between the I·U/U·I pairs in duplex 1, two kinks on either side of the tandem I·U wobbles of 19° and 27° in duplex 2 and 24° and 29° in duplex 3) appear to be quite significant. The kinks can be related to the roll and tilt angles in the duplexes (Table 2), which are at a maximum near the I·U/U·I mismatches. The structure was solved starting with the coordinates of the duplex r(CCCCGGGG)$_2$ (25) with a straight helical axis. The three independent duplexes could pack well in the unit cell without any bad contacts. In addition, the structure could not be refined with non-crystallographic symmetry restraints, indicating that the observed differences in the conformation of the three duplexes are real. To understand the role of packing forces on the observed bends, structures of the same sequence in different space groups should be studied.

The average minor groove widths for the present three duplexes involving I·U/U·I wobbles are 10.1, 9.8 and 9.9 Å, respectively, for five measurements. At the middle of duplexes 2 and 3, the grooves get constricted to 9.4 and 9.1 Å, respectively. Similar constricted minor groove widths have been observed for octamers with tandem purine·pyrimidine mismatches, G·U/U·G(21) and U·G/G·U (22), and C·A$^+$/A$^+$·C mismatches (15). This may be compared with the canonical A-RNA (11.1 Å). The Watson–Crick octamer, r(CCCCGGGG) (25), which was used as the search model for structure solution also has comparable minor groove widths, ranging from 9.6 to 10.0 Å. Therefore, the wobbles and the Watson–Crick base paired octamers have similar minor groove widths. This indicates that the tandem wobbles can be incorporated without significantly perturbing the duplexes. Major groove width was not considered because only one measurement is possible for an octamer.

I·U wobbles

The I·U mispairs adopt the same wobble base pairing (Fig. 3a). Each I·U base pair has two hydrogen bonds: N3(U)···O6(I) (average 2.84 Å) and N1(I)···O2(U) (average 2.79 Å) (Table 3a). In all three duplexes the C1′–C1′ distances of the I·U wobble pairs are very similar to the G·U wobble pair (21,22,29,30) and the Watson–Crick A·U/G·C pairs (10.5–10.7 Å), but the angles λ1 and λ2 (definitions of λ1 and λ2 and values are given in Table 3b) of the wobbles are asymmetric. However, a bridging water molecule invariably found in G·U pairs connecting the 2-amino group of guanosine and the O2 of uridine, which also hydrogen bonds to the 2′-hydroxyl group of the same uridine, are not present in I·U wobbles. The thermal parameters (B factors) for the I·U pairs (average 30.0 Å^2) are very similar to that of the Watson–Crick base pairs (average 30.9 Å^2), indicating similar mobility for the mismatched base pairs and the Watson–Crick pairs. Similar observations have been made in tandem mismatches U·G/G·U (motif I)(22) and G·U/U·G (motif II) (21) by our computation and also RNA duplexes incorporating other mismatches (15,29,30).

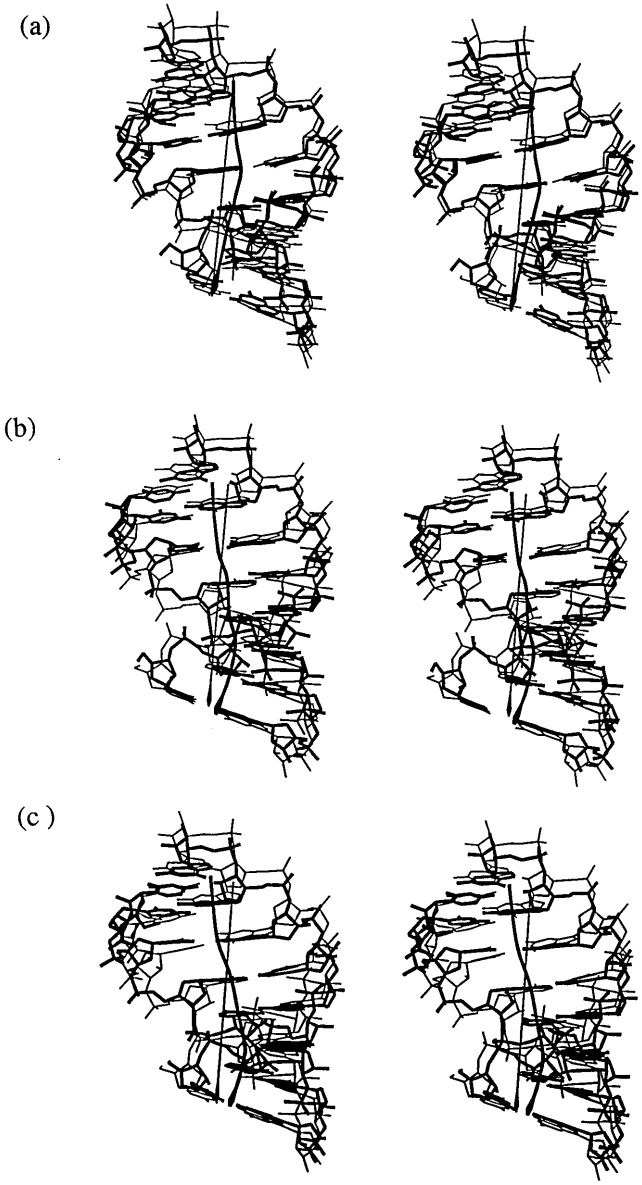

Figure 2. Stereoviews of the curvature of the helical axes in the three independent duplexes (thick lines), (**a**) duplex 1, (**b**) duplex 2 and (**c**) duplex 3, compared with the model of fiber A-RNA (thin lines).

Table 3a. Parameters for the I·U mismatches: hydrogen bond distance (Å)

Hydrogen bonds	Duplex 1	Duplex 2	Duplex 3
4N1(I)···13O2 (U)	2.79	2.81	2.77
13N3 (U)···4O6 (I)	2.91	2.73	2.76
12N1(I)···5O2 (U)	2.75	2.81	2.78
5N3(U)···12O6 (I)	2.85	2.87	2.93

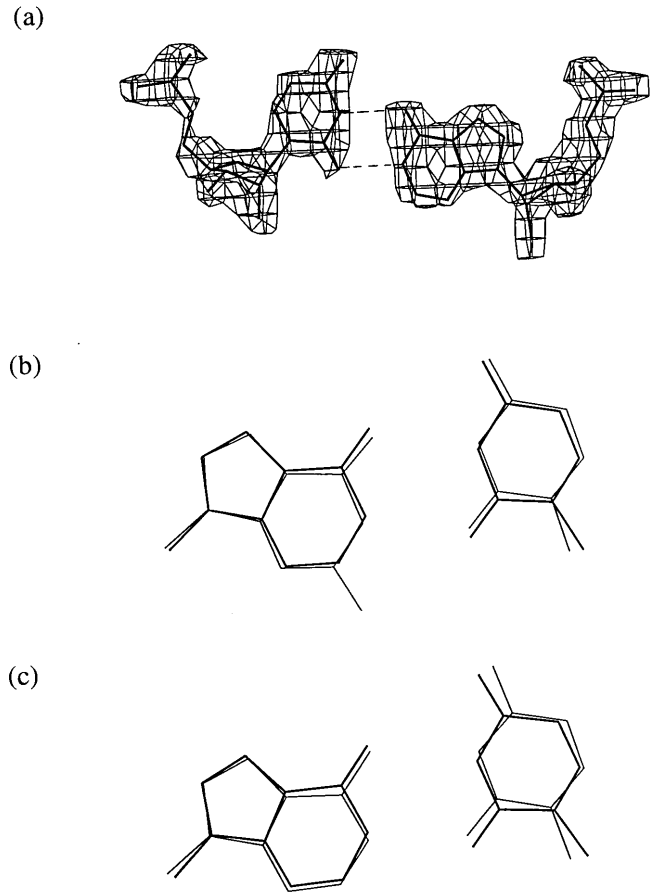

Figure 3. (**a**) The final $2|F_o|-|F_c|$ electron density map for the I4·U13 base pair in duplex 1 with their coordinates superimposed. The contours are at 1.0 σ. Similar density maps are observed for the other I·U base pairs. Comparison of the geometry of the I·U wobble pair with G·U wobble (**b**) and A·C wobble (**c**) pairs (14).

Table 3b. Parameters for the I·U mismatches: C1′–C1′ distances and angles between glycosidic bonds and the C1′–C1′ vector

	Base pair	λ1 (°)[a]	λ2 (°)[a]	Distance (Å)
Duplex 1	I4·U13 (wobble)	46.2	56.9	10.57
	U5·I12 (wobble)	42.5	61.5	10.51
Duplex 2	I4·U13 (wobble)	44.2	60.4	10.29
	U5·I12 (wobble)	53.9	60.5	10.43
Duplex 3	I4·U13 (wobble)	44.9	59.5	10.55
	U5·I12 (wobble)	43.8	60.0	10.59
Average		45.9	59.8	10.49
ApU (33)	A·U (W-C)	56	57	10.4

[a]λ1 is the angle N9(I)–C1′(I)–C1′(U) and λ2 is the angle N1(U)–C1′(U)–C1′(I).

Superimposition of the 4 bp involving the I·U/U·I base pairs and the flanking C·G/G·C base pairs with canonical RNA shows three different arrangements of the tandem I·U wobbles (Fig. 4). In Figure 4a, inosine rotates toward the minor groove while uracil

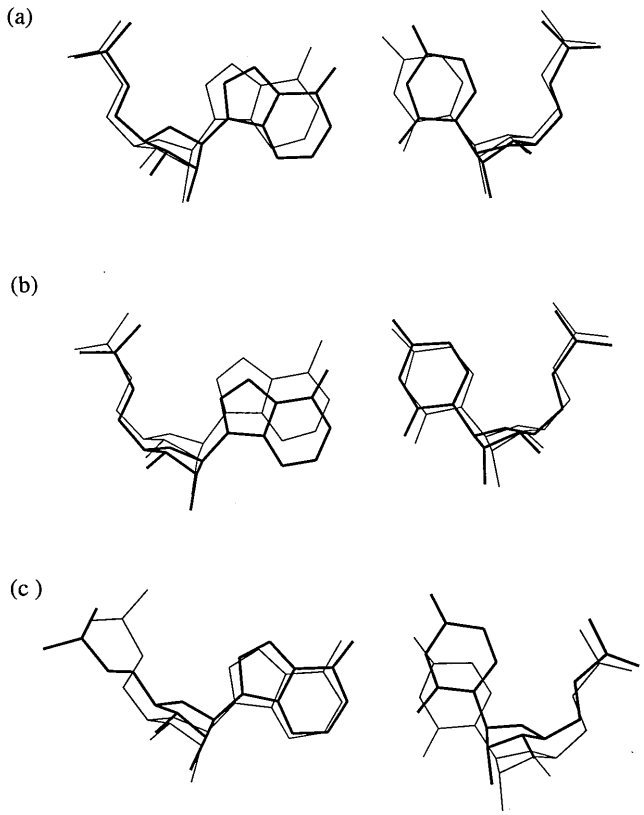

Figure 4. Three different patterns for the movements of the wobble bases as observed on superimposition of the I·U wobbles (thick lines) on the Watson–Crick A·U base pairs (thin lines). (**a**) I4 · U13 in duplex 1, (**b**) U5 · I12 in duplex 1 and (**c**) I·U wobbles in duplexes 2 and 3.

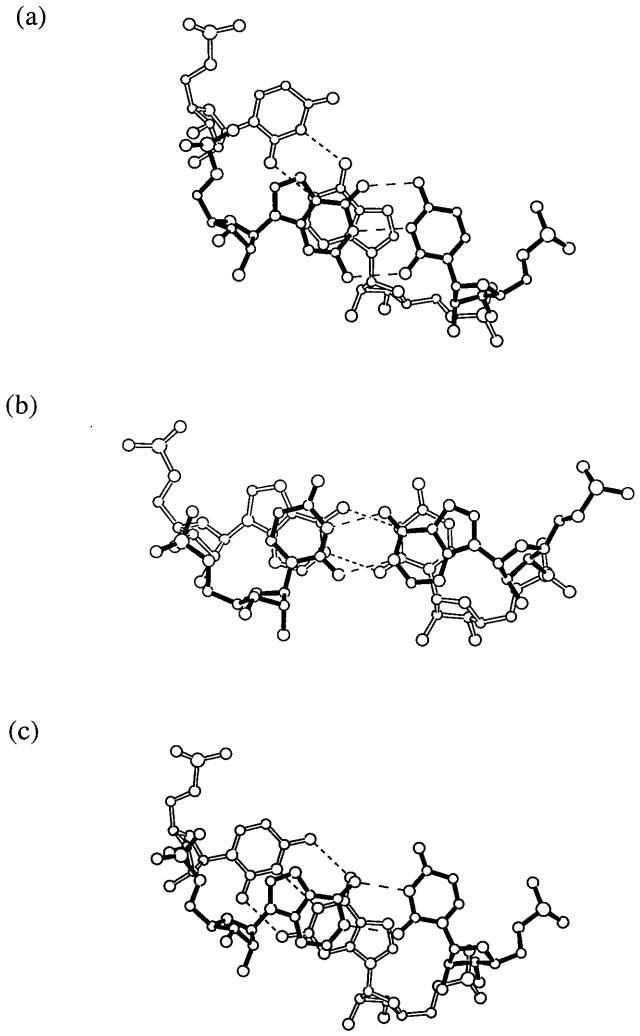

Figure 5. Base pair stacking for (**a**) the I·U wobble pair with the flanking C·G Watson–Crick pair on the 5′-side: C3·G14 (filled bonds) and I4·U13 (open bonds), (**b**) the central tandem I·U base pairs: I4·U13 (filled bonds) and U5·I12 (open bonds) and (**c**) the I·U wobble pair with the flanking C·G Watson–Crick pair on the 3′-side: U5·I12 (filled bonds) and G6·C11 (open bonds) in duplex 2. The stacking patterns are similar in duplexes 1 and 3.

rotates toward the major groove without translation of the bases as first observed in the crystal structure of d(CCIGGCCm^{5}CGG) (31); in Figure 4b, inosine translates toward the minor groove while uracil is almost unchanged; in Figure 4c, inosine remains in the same position while uracil translates toward the major groove with slight rotation. It is thought that in the wobbles, the purine is translated towards the minor groove while the pyrimidine is translated towards the major groove (13).

The twist angles and the rise for the I-U step decrease in two of the three independent molecules (24.4° and 2.3 Å for duplex 2; 26.5° and 2.5 Å for duplex 3). Figure 5 shows the base stacking for the two tandem I·U wobble base pairs. The tandem wobbles stack with intrastrand purine-pyrimidine overlap (Fig. 5b) and with the flanking C·G base pairs they stack with interstrand purine-purine overlap (Fig. 5a and c), which leaves the uracil and cytosine bases unstacked and available for interaction with other ligands. The stacking of the I·U wobble pairs in all three duplexes is similar despite the large difference in the twist angles which arise from different kinks in the three duplexes. Thus, based on the stacking consideration, I·U pairs should be expected to be similar in stability to G·U pairs. However, G·U pairs are more stable because of the bridging water molecule (21,32). The important stability of the G·U wobble contributed by water-mediated hydrogen bonding may explain the thermodynamic data (19).

Structural information on the sequences U·G/G·U (motif I)(22) and G·U/U·G (motif II) (21) are known from our earlier work. U·G/G·U wobble pairs display interstrand purine-purine stacking leaving the two pyrimidines unstacked. In the reverse motif, G·U/U·G, both wobble base pairs are stacked. However, motif I stacks with the flanking Watson–Crick base pairs but motif II leaves the uridine unstacked. The unstacked bases can provide a platform for recognition by proteins or other ligands. At present, structural information for only one motif I·U/U·I, motif II (present structure) and C·A$^+$/A$^+$·C in motif I (15) is available. We have found similar base stacking patterns for the same motifs; stacking of the tandem I·U/U·I pairs and the flanking Watson–Crick base pairs are very similar to G·U/U·G. Similarly, stacking of the tandem U·G/G·U wobble and the flanking Watson–Crick base pairs are the same as that for C·A$^+$/A$^+$·C. Based on the similarities of stacking for the same motif, we may expect that U·I/I·U will have a similar recognizable surface to U·G/G·U (motif I).

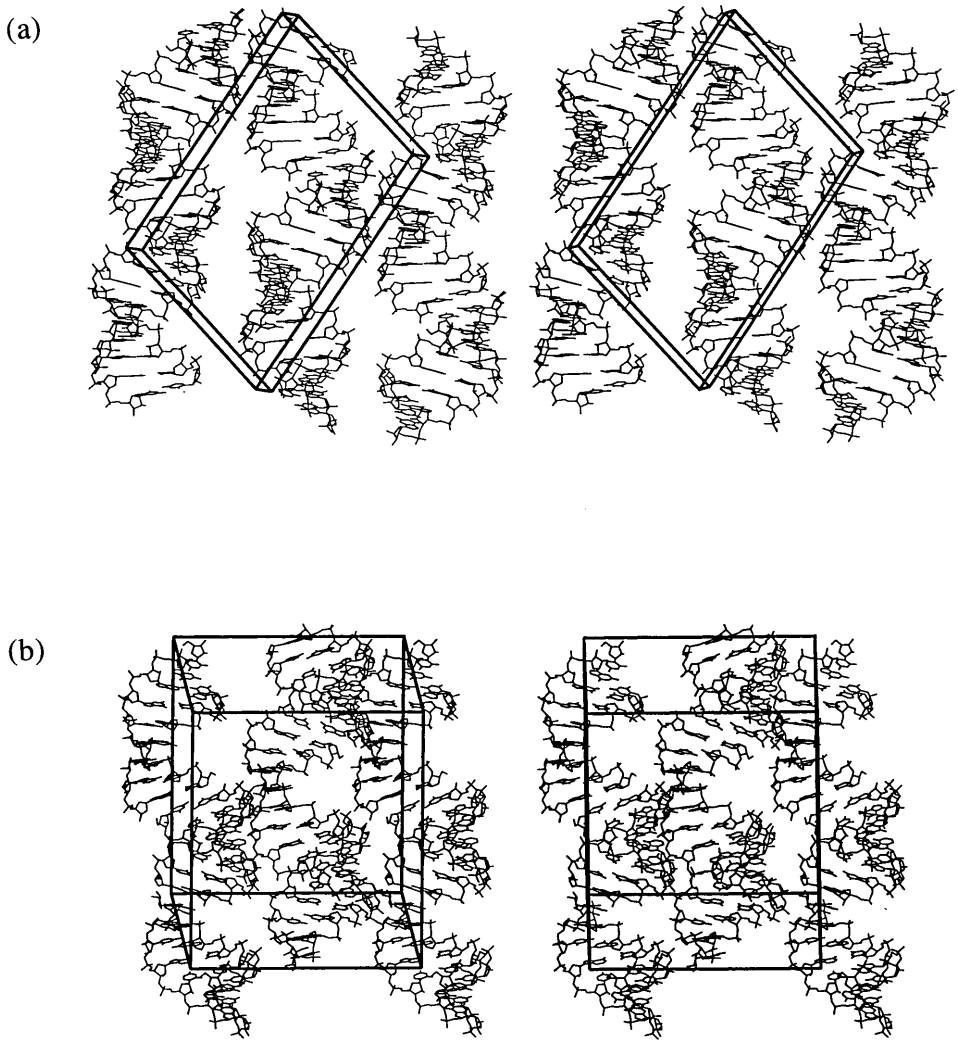

Figure 6. Crystal packing showing (**a**) the interactions with translationally related columns and (**b**) the 2_1-screw related columns.

Crystal packing and hydration

The three independent duplexes are stacked one behind the other in a pseudo-continuous helical packing approximately along the *a*–*c* diagonal (Fig. 6). The twist and rise are 5.23° and 2.52 Å at the junction step between duplexes 1 and 2, 9.33° and 2.72 Å between 2 and 3 and 33.84° and 2.64 Å between 3 and 1. The twist angles at the former two junction steps are low while that of the latter is close to the values for the other base pair steps in the duplexes. The distance between the interhelical columns is ~22 Å and the duplexes are packed tightly, with a volume/bp of 1400 Å^3. Molecules (columns) in space group $P2_1$ can interact through translation symmetry along the *a*, *b* and *c* axes and with 2_1-screw axis related molecules; in the present packing the minor groove of one column faces the backbone of an adjacent column (Fig. 6). Each helical column is surrounded by six columns in a pseudo-hexagonal packing arrangement. The tight crystal packing allows only 26 water molecules to be located. Most of the water molecules are hydrogen bonded to 2′- and terminal 3′-hydroxyl groups, phosphate groups and major and minor groove base atoms.

The 2′-hydroxyl groups participate in both interduplex (or intercolumn) and intraduplex interactions. There are 16 interduplex hydrogen bond interactions involving: O2′-O2P, O2′-O4′, O2′-O3′, O2′-O2′ and O2′-base (Table 4a). The preponderant interactions are with O2P of the phosphate groups which point in a direction away from the major groove. It is important to point out that half of the 2′-hydroxyl groups in the six I·U wobbles participate in interduplex interactions. There are 17 intrastrand O-H···O hydrogen bonding interactions involving 2′-hydroxyl groups with O4′ and O5′ of the next (I+1) residue (Table 4b).

In conclusion, I·U/U·I wobble pairs can be incorporated into RNA duplexes without significant distortion of the helix and may explain why they occur frequently in biological RNAs. The overall geometry of the tandem I·U wobble pairs resembles closely the tandem G·U and A^+·C wobble pairs. The base stacking patterns of these wobble pairs with the flanking sequences allow similar disposition of the bases in the grooves for interactions

with proteins. This appears to be the structural basis as to why I·U can substitute for a G·U pair in some rRNAs. We are of the opinion that I·U, G·U and A^{+}·C wobbles isolated by Watson–Crick base pairs would have similar characteristic geometries and stacking patterns and may substitute for each other in a duplex.

Table 4a. Interduplex interactions (≤3.40 Å) of 2′-hydroxyl groups

2′-Hydroxyl	Atom (residues)	Distance (Å)
G7 (duplex 1)	O2P (I12, duplex 2)	2.72
G14 (duplex 1)	O2P (G7, duplex 2)	2.68
I4 (duplex 2)	O2P (G16, duplex 3)	2.65
G8 (duplex 2)	O2P (G7, duplex 3)	3.02
U13 (duplex 2)	O2P (G6, duplex 1)	2.47
I4 (duplex 3)	O2P (G16, duplex 2)	2.26
U13 (duplex 3)	O2P (I12, duplex 2)	2.86
G15 (duplex 2)	N2 (G14, duplex 3)	3.15
G6 (duplex 3)	N2 (G7, duplex 2)	3.15
G15 (duplex 3)	N2 (G14, duplex 2)	3.07
G7 (duplex 2)	O2′ (G7, duplex 3)	3.20
I12 (duplex 2)	O2′ (I12, duplex 3)	3.33
G16 (duplex 2)	O2′ (C3, duplex 3)	2.72
C3 (duplex 3)	O3′ (G16, duplex 2)	3.17
I12 (duplex 1)	O4′ (C11, duplex 3)	3.31
C11 (duplex 2)	O4′ (G6, duplex 3)	3.19

Table 4b. Intrastrand interactions (≤3.40 Å) of 2′-hydroxyl groups

2′-Hydroxyl	Atom (residues)	Distance (A)
Duplex 1		
C1	O4′ (C2)	3.20
C3	O4′ (I4)	2.68
U5	O4′ (G6)	2.93
U5	O5′ (G6)	3.10
G6	O5′ (G7)	3.18
G7	O5′ (G8)	3.16
U13	O5′ (G14)	3.13
G14	O5′ (G15)	3.37
Duplex 2		
U5	O4′ (G6)	3.32
U13	O5′ (C14)	3.26
G14	O5′ (G15)	3.27
G15	O4′ (G16)	3.38
Duplex 3		
C3	O5′ (I4)	3.25
C11	O4′ (I12)	3.27
U13	O4′ (G14)	3.28
U13	O5′ (G14)	3.17
G15	O5′ (G16)	3.26

The stability of the Watson–Crick A·U pair compared with the I·U wobble pair can be explained based solely on the stacking. Each of the base pairs has two hydrogen bonds but the loss of stacking of I·U pairs with the flanking base pairs (as observed here) could be significant enough to explain the greater thermodynamic stability of the A·U pair compared with the I·U pair. The I·U pair is less stable than the G·U pair because of the extra water-mediated hydrogen bonding of the 2-amino group of guanine. This may be the reason why G·U pairs are more abundant compared with the other wobble pairs.

ACKNOWLEDGEMENTS

M.S. thanks the Board of Regents for an Ohio Eminent Scholar Chair. We gratefully acknowledge the National Institutes of Health for grant GM-17378 and an Ohio Eminent Scholar Endowment for supporting this work. We also thank the Hayes Investment Fund of the University for partial support to purchase the R-axis IIc imaging plate.

REFERENCES

1 Limbach,P.A., Crain,P.F. and McCloskey,J.A. (1994) *Nucleic Acids Res.*, **22**, 2183–2196.
2 Sprinzl,M., Steegborn,C., Hubel,F. and Steinberg,S. (1996) *Nucleic Acids Res.*, **24**, 68–72.
3 Bass,B.L. and Weintraub,H. (1988) *Cell*, **55**, 1089–1098.
4 Wagner,R.W., Smith,J.E., Cooperman,B.S. and Nishikura,K. (1989) *Proc. Natl Acad. Sci. USA*, **86**, 2647–2651.
5 Melcher,T., Mass,S., Higushi,M., Keller,W. and Seeburg,P.H. (1995) *J. Biol. Chem.*, **270**, 8566–8570.
6 Yang,J., Sklar,P., Axel,R. and Manlatis,T. (1995) *Nature*, **374**, 77–81.
7 Rueter,S.M., Burns,C.M., Coode,S.A., Mookherjee,P. and Emerson,R.B. (1995) *Science*, **267**, 1491–1494.
8 Melcher,T., Mass,S., Herb,A., Sprengel,R., Seeburg,P.H. and Higuchi,M. (1996) *Nature*, **379**, 460–464.
9 Ecker,A., ter Meulen,V., Baczko,K. and Schneider-Schaulies,S. (1995) *J. Neurovirol.*, **1**, 92–100.
10 Horikami,S.M. and Moyer,S.A. (1995) *Virus Res.*, **36**, 87–96.
11 Polson,A.G., Bass,L. and Casey,L.C. (1996) *Nature*, **380**, 454–456.
12 Sharmeen,L., Bass,B., Sonenberg,N., Weintraub,H. and Groudine,M. (1991) *Proc. Natl Acad. Sci. USA*, **88**, 8096–8100.
13 Crick,F.H.C. (1966) *J. Mol. Biol.*, **19**, 548–555.
14 Pan,B., Mitra,S.N. and Sundaralingam,M. (1998) *J. Mol. Biol.*, **283**, 977–984.
15 Jang,S.B., Hung,L.-W., Chi,Y.-I., Holbrook,E.L., Cater,R.J. and Holbrook,S.R. (1998) *Biochemistry*, **37**, 11726–11731.
16 Gutell,R.R., Larsen,N. and Woese,C.R. (1994) *Microbiol. Rev.*, **58**, 10–26.
17 Michel,F., Umesono,K. and Ozeki,H. (1989) *Gene*, **82**, 5–30.
18 Michel,F. and Westhof,E. (1990) *J. Mol. Biol.*, **216**, 585–610.
19 Strobel,S.A., Cech,T.R., Usman,N. and Beigelman,L. (1994) *Biochemistry*, **33**, 13824–13835.
20 Bass,B.L. and Weintraub,H. (1987) *Cell*, **48**, 607–613.
21 Biswas,R. and Sundaralingam,M. (1997) *J. Mol. Biol.*, **270**, 511–519.
22 Biswas,R., Wahl,M.C., Ban,C. and Sundaralingam,M. (1997) *J. Mol. Biol.*, **267**, 1149–1156.
23 Green,R., Szostak,J.W., Benner,S.A., Rich,A. and Usman,N. (1991) *Nucleic Acids Res.*, **19**, 4161–4166.
24 Navaza,J. (1994) *Acta Crystallogr.*, **A50**, 157–163.
25 Portmann,S., Usman,N. and Egli,M. (1995) *Biochemistry*, **34**, 7569–7575.
26 Brunger,A.T. (1992) *XPLOR Manual*, v.3.0. Yale University Press, New Haven, CT.
27 Berman,H.M., Olson,W.K., Beveridge,D.L., Westbrook,J., Gelbin,A., Demeny,T., Hsieh,S.H., Srinivasan,A.R. and Schneider,B. (1992) *Biophys. J.*, **63**, 751–759.
28 Lavery,R. and Sklenar,H. (1989) *J. Biomol. Struct. Dyn.*, **4**, 655–667.
29 Holbrook,S.R., Cheong,C., Tinoco,I.,Jr and Kim,S.-H. (1991) *Nature*, **353**, 579–581.
30 Baeyens,K.J., Debondt,H.L. and Holbrook,S.R. (1995) *Nature Struct. Biol.*, **2**, 56–63.
31 Ramakrishnan,B. and Sundaralingam,M. (1995) *Biophys. J.*, **69**, 553–558.
32 Betzel,C., Lorenz,S., Futste,J.P., Zhang,M., Schneider,T.R., Wilson,K.S. and Erdmann,V.A. (1994) *FEBS Lett.*, **351**, 159–164.
33 Seeman,N.C., Rosenberg,J.M., Suddath,F.L., Kim,J.J.P. and Rich,A. (1976) *J. Mol. Biol.*, **104**, 109–144.